Published by
NIGERIAN SOCIETY OF PHYSICAL SCIENCES
Available online @ https://asr.nsps.org.ng/index.php/asr

African Scientific Reports 3 (2024) 80

African Scientific Reports

On topological indices and QSPR analysis of some drugs used for treating Coronavirus patients

Hassan Ibrahim[a,*], Deborah Abolape Akwu[b], Reza Sharafdini[c]

[a]*Department of Mathematics, Federal University of Lafia, Makurdi Road Gandu, Lafia, PMB 146, Nigeria*
[b]*Department of Mathematics, Joseph Sarwuan Tarka University, North Bank, Makurdi, PMB 2373, Nigeria*
[c]*Department of Mathematics, Persian Gulf University, Bushehr, Iran*

Abstract

A topological index is a real number obtained from the molecular graph structure. It can predict the physicochemical and biological properties of many anticoronavirus drugs. In this article, the topological index of some drugs for the treatment of coronavirus was computed using the Wiener-Hosoya eigenvalues of the molecular structure of hydroxychloroquine, chloroquine, camostat, nafamostat, remdesivir, and lopinavir compounds, and the Quantitative Structure Property Relationship (QSPR) study of some properties: Boiling point, Molar weight, Flash point and Enthalpy were investigated. It was observed that the regression model value r is more than 0.6 and p value shows less than 0.05.

DOI:10.46481/asr.2024.3.2.80

Keywords: Energy, Eigenvalues, Molecular structures, QSPR

Article History:
Received: 29 December 2022
Received in revised form: 22 February 2024
Accepted for publication: 13 May 2024
Published: 31 May 2024

1. Introduction

A graphical index is a numerical value corresponding to a structural invariant graph, and in chemical graph theory, these invariants are known as topological indices. In the field of medical and chemical sciences, the topological indices are used for studying the chemical, medical, biological and pharmaceutical or physicochemical properties or features of drugs. Concerning the previous deadly diseases, the COVID-19 pandemic has been considered the biggest life-threatening issue that modern medicine has ever tackled. Scientists have tested available antiviral agents and got a favourable impact of recovering from pandemic. Highlighting the importance of topological indices in the study of pharmaceutical and chemical drugs, Jorge *et al.* [1] presented a mathematical pattern for the screening of the well-known viral protease inhibitor called lopinavir as the reference drug in treating COVID-19. Their results indicate that anitiviral such as Brecanavir, as well as virus groups of drugs among which are antibiotics of the microlide family (azithromycin, clarithromycin, erythromycin among others) could be useful in treating COVID-19 infection.

In the same year, Sayed *et al.* [2] investigated several degree-based and neighborhood degree-sum-based topological indices for several antiviral drugs using M-polynomials and neighborhood M-polynomials methods. In addition, a quantitative structure-property was established between the various topological indices and the various physiochemical properties of these antiviral drugs, along with

*Corresponding author: Tel.: +234-803-877-7558.
Email address: hifulafia@gmail.com (Hassan Ibrahim)

redesivir, chloroquine, hydroxychloroquine, and theaflavin was performed in order to access the efficacy of the calculated topological indices. The results obtained reveal that the topological indices under study have a strong correlation with the physicochemical characteristics of the potential antiviral drugs. They went further to investigate the biological activity ($P1C_{50}$) of these compounds using multiple linear regression (MLR) analysis.

Inspired by the work in Anand *et al.* [3], Hosamani [4] studied the quantitative-structure property relationship (QSPR) of phytochemicals screened against SARS-Cov-2 $3CL^{pro}$ with the help of topological indices like the first Zagreb index M_1, second Zagreb Index M_2, Randić index R, the Balban index, and the sum-connectivity index (SCI). The study revealed that SCI and M_1 are two important parameters to predict the molecular weight of the topological polar surface area of phytochemicals, respectively. Habibi and Taheri [5] selected a subset of human proteins as a candidate set that can bind to approved drugs. The method is based on the information about human virus- protein interaction and their effect in the biological processes on the host cells. Some informative topological and statistical features for proteins in the protein-protein interaction network were presented. Two groups of drugs was selected and evaluated. The first group contains the experimental unapproved treatment for COVID-19 and shows that, of the 17 drugs in this group, 15 drugs are approved by their selected sets. The second group contains the extended clinical trials for COVID-19. The COVID-19 associated protein sets were studied, and proteins that are essentially involved in disease pathology were also identified.

Mathematical models as an integral part of artificial intelligence are designed for contact tracing, genetic network analysis for uncovering the biological evolution of viruses, understanding the underlying mechanisms of the observed disease dynamics, evaluating mitigation strategies, and predicting the COVID-19 pandemic dynamics. Nandini *et al.* [6] described mathematical techniques to exploit and understand the progression of the pandemic through a theoretical characterization of the underlying graphs. They obtained several topological indices for the various graphs of biological interest, such as pandemic trees, Cayley trees, Christmas trees, and the Corona product of Christmas tree and paths. The plots of entropy and logarithms of topological indices of pandamic trees accentuate the underlying severity of COVID-19 over the 1918 Spanish flu pandemic.

Abdul *et al.* [7] computed the topological indices based on even-degree and negative-degree for the Hydroxythyl Starch and Hydroxychroroquine (HCQ-HEC) biconjugate molecular structures. Ev-degree and ve-degree based topological indices are two novel degree-based indices as defined in graph theory. They are defined as responding to their relating partners. Wei *et al.* [8] went further to compute some reverse topological indices, namely the reverse general Randić index, the reversed atom-bond connectivity index, the reverse geometric arithmetic index, the reversed forgotten index, the reversed Balaban index, and the reverse Zagreb type indices of some of the molecular structure of anitiviral drugs in treating COVID-19. In their computations, indices showed higher values for Remdesivir. Anwar *et al.* [9] computed the Reduced Neighborhood topological indices and RNM-polynomials of some of the antiviral agents. In particular, they considered Remdesivir, Chloroquine, Hydroxychloroquine, Theaflavin, and Dexamethason. They went further to evaluate the RNM-polynomials of these structures with 3D graphical representations.

At the point when topological descriptors are joined with another quantum chemically determined electronic parameter, for example, highest occupied molecular orbital, the lowest unoccupied molecular orbital, the energy of graphs, hardness, polarizability, atomic electrostatic potentials, natural bond orbital investigations, and so on, one could get quantitative proportions of the reactiveness, stability, and binding potentials of a drug. In light of this, Liu *et al.* [10] derived the quantitative structure properties of several antiviral drug compounds used to fight the outbreak of COVID-19. Their method of computation was based on the identification of suitable edge-cuts such that the resulting graph leaves many convex components, which enabled them to formulate some required properties. A graphical representation of some computed topological indices such as Wiener, Szeged, and Mostar and their variants was shown.

Topological indices are important attributes to analyze the physicochemical characteristics of chemical compound structures.There are five different types of topological indices: degree, distance, eigenvalue, matching, and mixed. In the above literature, all the topological indices used are degree-based. Pharmaceutical research, which has to do with going to the laboratory, is time-consuming and cost-effective, hence there is a need to devise another way to study the efficacy and efficiency of drugs. In this study, we shall compute the topological indices based on the Wiener-Hosoya matrix of the molecular structure proposed by Hassan *et al.* [11], which is both vetex-degree and distance-based, of some antiviral drugs for the treatment of COVID-19 and construct a QSPR model.

This notion of Wiener-Hosoya index can serve as a topological index in chemical graph theory for Quantitative Structure Property Relationship (QSPR) and Quantitative Structure Activity Relationship (QSAR) studies by predicting the physiochemical properties of the chemical structure of drugs and other chemical compounds. This energy can be used to investigate the coherence of connected graphs.

2. Materials and methods

2.1. The Wiener-Hosoya topological index

Let G be a connected graph with vertices $v_i (i = 1, 2, \cdots, n)$ and $v_j (j = 1, 2, \cdots, n)$. Then, the transmission of a vertex $v_i \in G$, denoted as $\sigma_i = \sigma_G(v_i)$, is given as [12]

$$\sigma_i = \sigma_G(v_i) = \sum_{i=1}^{n} d_G(v_i, v_j). \tag{1}$$

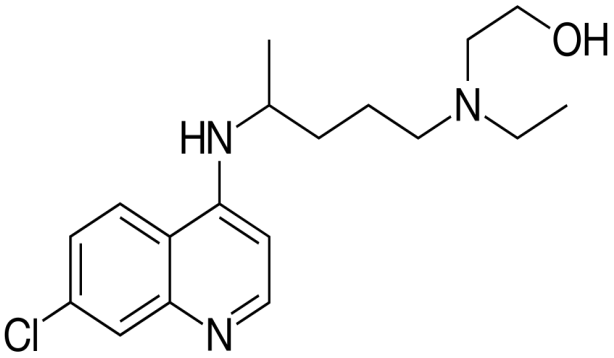

Figure 1: Chemical structure of Hydroxychloroquine ($C_{18}H_{26}CIN_3O$).

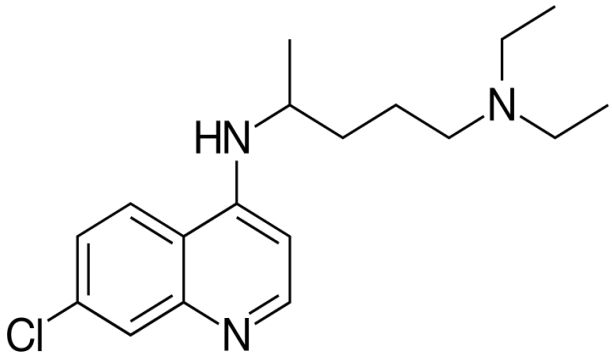

Figure 2: Chemical structure of Chloroquine ($C_{18}H_{26}CIN_3$).

The Wiener index of G, denoted by $W(G)$, has the following representations:

$$W(G) = \frac{1}{2}\sum_{i=1}^{n}\sum_{j=1}^{n} d_G(v_i, v_j) = \frac{1}{2}\sum_{i=1}^{n}\sigma_i = \sum_{i\sim j}\left(\frac{\sigma_i}{2d_i} + \frac{\sigma_j}{2d_j}\right). \tag{2}$$

It is obvious that $\frac{\sigma_i}{2d_i} + \frac{\sigma_j}{2d_j}$ is positive, and the function,

$$w : E(G) \longmapsto \mathbb{R}^+ v_i v_j \longmapsto \frac{\sigma_i}{2d_i} + \frac{\sigma_j}{2d_j}, \tag{3}$$

is a weight function on $E(G)$. This weight function is called Wiener-Hosoya weighting. The adjacency matrix of G with respect to the Wiener-Hosoya weighting in equation (3) is denoted by $\mathbb{WH}(G) = (w_{i,j})$, where in Ref. [11], we have the following:

$$w_{i,j} = \begin{cases} \frac{\sigma_i}{2d_i} + \frac{\sigma_j}{2d_j} & i \sim j; \\ 0 & otherwise. \end{cases} \tag{4}$$

The Wiener-Hosoya energy of a graph G is the sum of the absolute values of its Wiener-Hosoya eigenvalues (see Ref. [11]), that is,

$$\varepsilon_{\mathbb{WH}(G)} = \sum_{i=1}^{n} |\lambda_i| . \tag{5}$$

2.2. The regression model

The regression model,

$$P = A + B\mathbb{WH}(G), \tag{6}$$

where P is the physical property of the drug, A is a constant, and B is the regression coefficient, and $\mathbb{WH}(G)$ represents the Wiener-Hosoya energy of a molecular graph, G, which will be used in this work for the purpose of numerical calculations. These values will be calculated using the R programming language for the values of four physical properties and the Wiener-Hosoya energy of the anticovid-19 drugs, as shown in Figures 1 to 6.

2.3. Molecular structure of some anti-Covid 19 drugs.

The chemical structures of hydroxychloroquine, chloroquine, lopinavir, remdesivir and nafamostat are depicted in Figures 1 to 6. Examining the physicochemical properties of these drugs is valuable.

3. Results and discussion

We applied the Wiener-Hosoya index on the chemical structures depicted in Figure 1 to 6, with their QSPR analyzed. The correlation between the characteristics of this index with some physicochemical characteristics of the drugs will also be showcased.

3.1. Molecular graph of the chemical drug compounds

The molecular graphs of the chemical structure of the drugs in Figures 1 and 2 are obtained by representing the atoms as the vertices and the bonds between them as the edges.

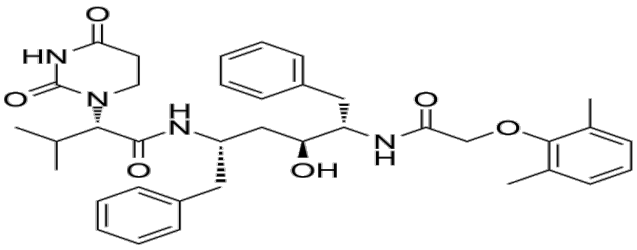

Figure 3: Chemical structure of Lopinavir ($C_{37}H_{48}N_4O_5S_2$).

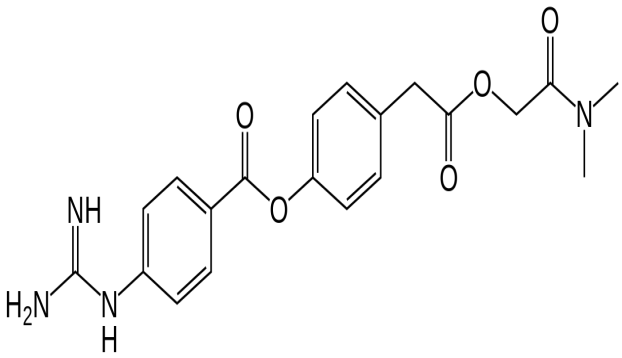

Figure 4: Chemical structure of Camostat ($C_{20}H_{22}N_40_5$).

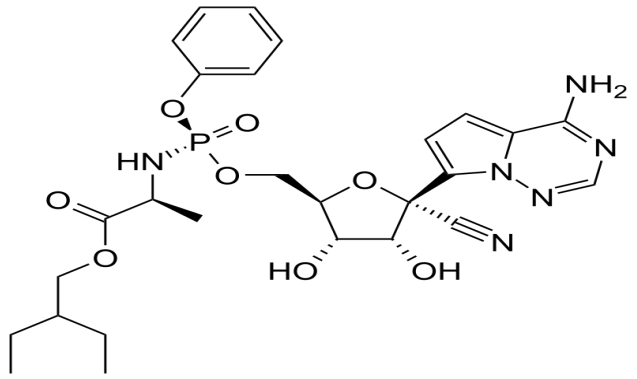

Figure 5: Chemical structure of Remdesivir ($C_{27}H_{35}N_6O_8P$).

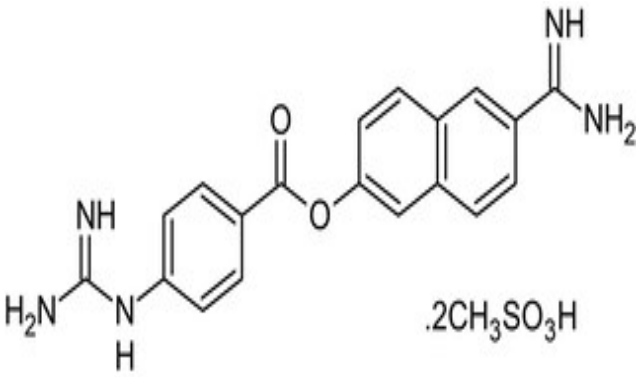

Figure 6: Chemical structure of Nafamostat ($C_{19}H_{17}N_5O_2$).

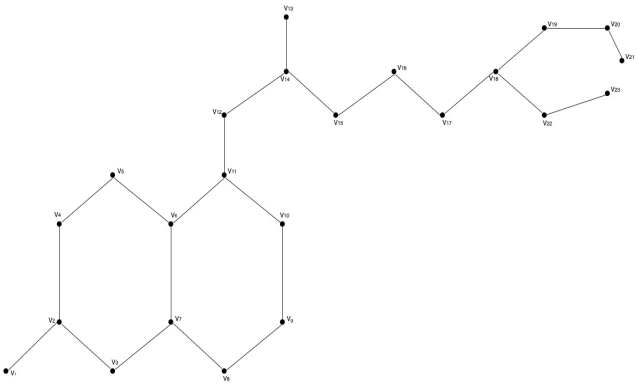

Figure 7: Molecular graph of Hydroxychloroquine anticovid-19 drugs.

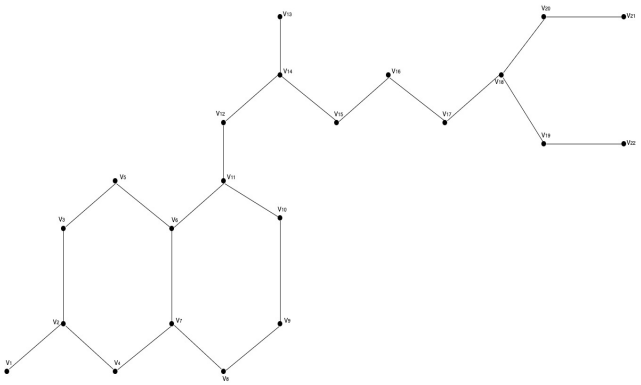

Figure 8: Molecular graph of Chloroquine anticovid-19 drugs.

3.2. *Computation of the vertex transmission of the molecular graphs*

The vertex transmission of the molecular graphs in Figures 7 - 12 was computed. See Tables A.1 to A.4 in the Appendix.

Theorem 1. *Let H_1, H_2, H_3, H_4, H_5, and H_6 be molecular graphs of chloroquine, hydroxychloroquine, camostat, nafamostat, remdesivir, and lopinavir compounds, respectively. Then,* $\mathbb{WH}(H_1) = 1573.6547$, $\mathbb{WH}(H_2) = 1843.3820$, $\mathbb{WH}(H_3) = 3721.4581$, $\mathbb{WH}(H_4) = 2517.0266$, $\mathbb{WH}(H_5) = 6389.5017$, *and* $\mathbb{WH}(H_6) = 10653.1564$.

Proof

The sum-transmission of vertices of the molecular graph of these compounds are given in Tables A.1 to A.4. The results are obtained by using equation 3.

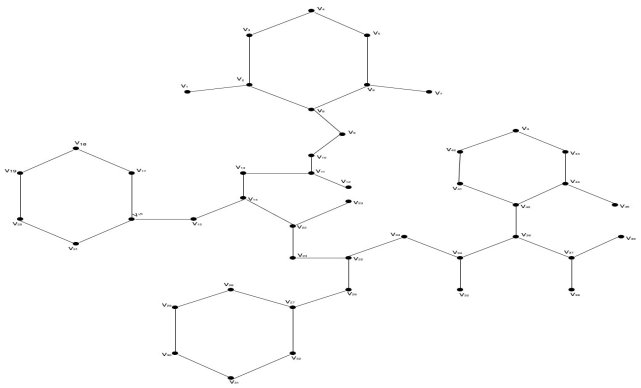

Figure 9: Molecular graph of Lopinavir anticovid-19 drugs.

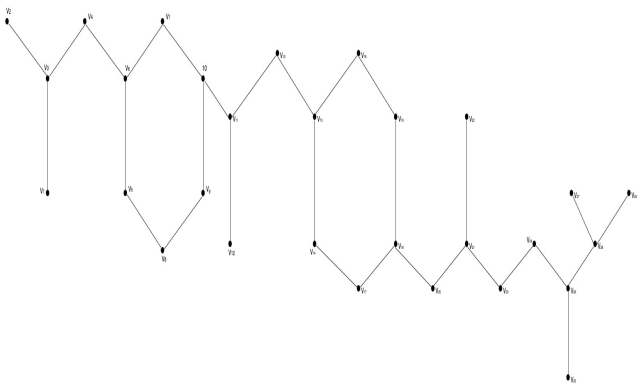

Figure 10: Molecular graph of Camostat anticovid-19 drugs.

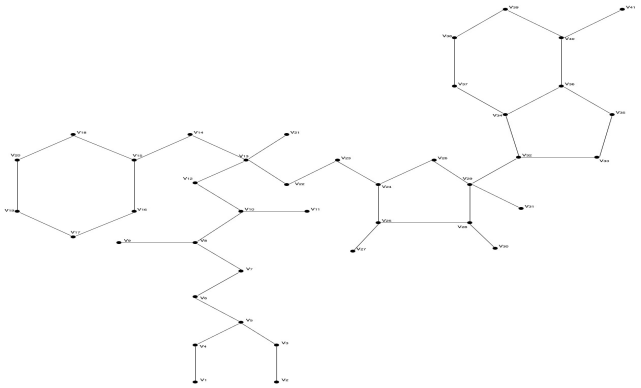

Figure 11: Molecular graph of Remdesivir anticovid-19 drugs.

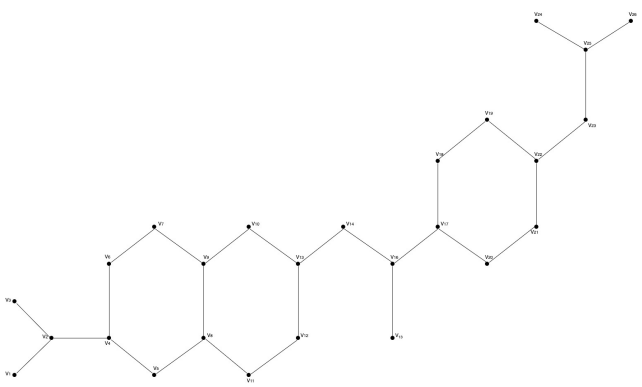

Figure 12: Molecular graph of Nafamostat anticovid-19 drugs.

Table 1: Various anticovid-19 drugs with its physiochemical properties.

SN	Drugs	Boiling Point	Molar Weight	Flash Point	Enthalpy
1	Chloroquine	289	-	259.6	75.1
2	Hydroxychloroquine	90	335.9	296.4	86.0
3	Camostat	155	389.4	337.6	-
4	Nafamostat	260	347.4	339.1	97.1
5	Remdesivir	-	602.6	-	-
6	Lapinovir	118	-	546.9	143.0

3.2.1. Linear QSPR models for the Wiener-Hosoya index

Using the regression model in Equation (6), we get the linear QSPR models for the Wiener-Hosoya index. Let BP denotes the boiling point, E, the enthalpy, MW, represents the molar weight,and FP, the flash point of the drugs. The QSPR model for the Wiener-Hosoya index for some properties of anticoronavirus drugs is;

$$\begin{aligned} BP &= 449.632 + 0.046\mathbb{WH}(G), \\ MW &= 271.725 + 0.038\mathbb{WH}(G), \\ FP &= 225.700 + 0.028\mathbb{WH}(G), \\ E &= 74.862 + 0.006\mathbb{WH}(G). \end{aligned}$$

The Table 1 shows the values of the Boiling Point, Molar weight, Flash Point and Enthalpy of the anticovid-19 drugs. Table 2 and Theorem 1 show the correlated values of the physicochemical properties of anticovid-19 drugs with Wiener-Hosoya energy. It can be observed that the Wiener-Hosoya energy, $\mathbb{WH}(G) = 0.937$, shows a higher significant positive correlation with molar weight when compared with other properties of the anticancer drugs. Similarly, $\mathbb{WH}(G) = 0.994$, shows highest the correlated value with

Table 2: Statistical parameters of the linear QSPR model for the Wiener-Hosoya index of anticovid-19 drugs.

Physical Properties	N	A	b	r	F	P	Indicator
Boiling Point	5	449.632	0.046	0.962	36.844	0.009	Significant
Molar Weight	5	271.725	0.038	0.943	32.209	0.005	Significant
Flash Point	5	225.700	0.028	0.962	36.852	0.009	Significant
Enthalpy	5	274.862	0.026	0.994	38.374	0.002	Significant

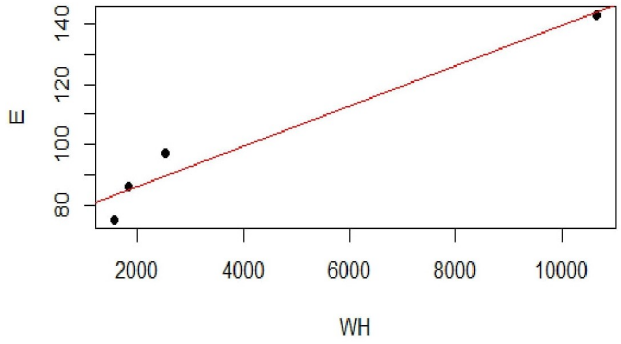

Figure 13: TI on enthalpy.

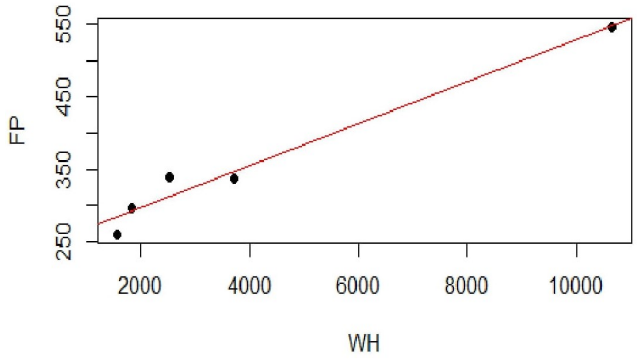

Figure 14: TI on flash point.

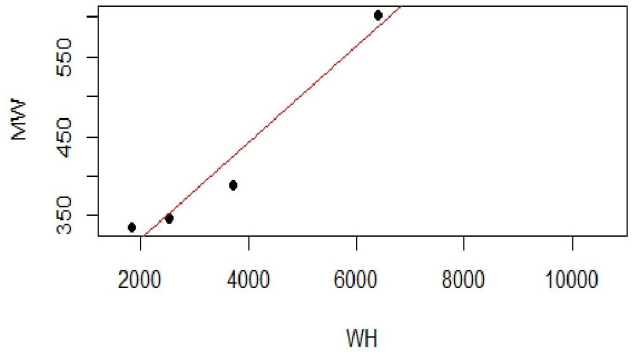

Figure 15: TI on molar weight.

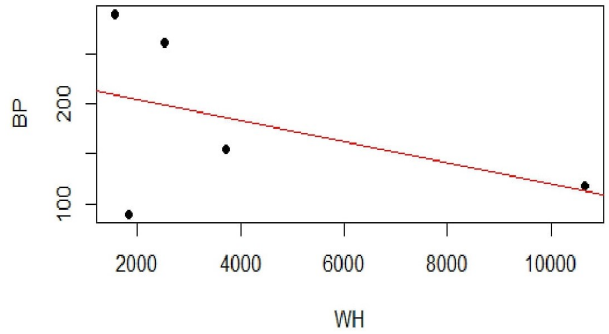

Figure 16: TI on boiling point.

Enthalpy compared with other properties of the anticovid-19 drugs. Table 2 shows the regression model of various physicochemical properties of anticovid-19 drugs.

Figures 7 to 8 depicts the molecular graphs of the chemical compounds in Figure 1 to 6, respectively. t shows that the graphs of these structures are single, connected and undirected. Each of the graph contains at least a cycle of order 6.

From our plots in Figure 13 to Figure 16, we can see a narrow spread of data points around the line which suggest a strong correlation between the properties and the topological index. The points also cluster closely around the lines, which suggests a strong linear relationship between these physicochemical properties and the Wiener-Hosoya index.

4. Conclusion

From our results, it was observed that the regression model value r is more than 0.6 and the p value shows less than 0.05. It therefore follows that all the physiochemical properties are highly significant. Unlike other topological indices, which are either degree-based or distance-based, we have shown that topological indecies based on mixed (degree and distance) can also be used to carry out a QSPR study of chemical compounds. A study may be carried out for different chemical structures, and a conclusion may be given based on their topological indices. May it be benzene structure, polymers, or any chemical compounds that can be taken for future study. A multi-disciplinary project may be taken up by researchers in various for a better result.

Acknowledgment

We thank the referees for they positive enlightening comments and suggestions, which have greatly helped us in making improvements to this paper. We also thank Prof. T. Aboiyar and Dr. S. T. Swem of Joseph Sarwuan Tarka University Makurdi for their constructive criticism and guidance to ensuring that this work is enhanced and accepted for publication. Our appreciation also goes to Dr. A. U. Abel of Chemistry Department, Federal University of Lafia, Nigeria for the proofreading of the manuscript.

References

[1] G. Jorge, R. Zanni & G. Maria, "Drugs repurposing for Coronavirus treatment", NEREIS **12** (2020) 15. https://doi.org/10.46583/nereis_2020.12.591
[2] A. Syed, P. Ali & F. Azam, "Topological indices and QSPR/QSAR analysis of some antiviral drugs being investigated for the treatment of COVID-19 patients", International Journal of Quantum Chemistry **22** (2020) 11. https://doi.org/10.1002/qua.26594.
[3] K. Anand, J. Ziebuhr & P. Wadhwani, "Coronavirus main proteins (3CLpro) structure basis for design of anti-SARS drugs", Journal of Science **300** (2003) 1763. https://doi.org/10.1126/science.1085658.
[4] S. Hosamani," Quantitative structure property analysis of anti-COVID-19 drugs", Journal of American Mathematical Society **90** (2020) 23. https://doi.org/10.48550/arXiv.2008.07350.
[5] M. Habibi & G. Taheri, "Topological network-based drug repurposing for Coronavirus", PLoS ONE **10** (2021) e0255270. https://doi.org/10.1371/journal.pone.0255270.
[6] G. Nandini, R. Rajan & A. Shatrinal, "Topological and thermodynamics entropy measures for COVID-19 pandamic through graph theory", Symmetry **24** (2021) 6. http://dx.doi.org/10.3390/sym12121992
[7] R. Abdul, M. Ishtiaq & M. K. Siddiqui, "Topological study of Hydroxychloroquine conjugated molecular structure used for novel Coronavirus (COVID-19) treatment", Polycyclic Aromatyic Compounds **6** (2021) 3792. https://doi.org/10.1080/10406638.2021.1873807
[8] J. Wei, M. Cancan, A. U. Rehman, M. K. Siddiqui, M. Nasir, M. T. Younas, M. F. Hanif, "On topological indices of remdesivir compound used for the treatment of Corona Virus (COVID-19)". Polycyclic Aromatic Compounds **42** (2022) 4300. http://doi.org/10.1080/10406638.2021.1887299.
[9] S. Anwar, G. Sophia & B. Dhananjayamurthy, "The revised neighborhood topological indices and RNM-polynomial for the treatment of COVID-19 ", Bionterface Research in Applied Mathematics **11** (2021) 11817. https://doi.org/10.33263/BRIAC114.1181711832
[10] J. Liu, M. Arockiaraj, T. Arulperumjothi & S. Prabhu, "Distance-based and bond-addictive topological indices of certain repurposed antiviral drugs compounds tested for treating COVID-19", International Journal of Quantum Chemistry **23** (2021) 21. https://doi.org/10.1002/qua.26617.
[11] H. Ibrahim, R. Sharafdini, T. Reti & A. Akwu, "Wiener-Hosoya matrix of connected graphs", Mathematics **9** (2021) 359. http://doi.org/10.3390/math9040359.
[12] R. Sharafdini & T. Reti, "On the transmission-based graph topological indices", Kragukevac Journal of Mathematics **44** (2020) 41. https://doi.org/10.48550/arXiv.1710.08176.

Appendix A.

Table A.1: Vertex transmission of Figure 7.

V	V_1	V_2	V_3	V_4	V_5	V_6	V_7	V_8	V_9	V_{10}	V_{11}	V_{12}	V_{13}	V_{14}	V_{15}	V_{16}	V_{17}	V_{18}	V_{19}	V_{20}	V_{21}	V_{22}	$\sum$
V_1	0	1	2	2	3	4	3	4	5	6	5	6	8	7	8	9	10	11	12	12	13	13	144
V_2	1	0	1	1	2	3	2	3	4	5	4	5	7	6	7	8	9	10	11	11	12	12	124
V_3	2	1	0	2	1	2	3	4	5	4	3	4	6	5	6	7	8	9	10	10	11	11	114
V_4	2	1	2	0	3	2	1	2	3	4	3	4	6	5	6	7	8	9	10	10	11	11	110
V_5	3	2	1	3	0	1	2	3	4	3	2	3	5	4	5	6	7	8	9	9	10	10	100
V_6	4	3	2	2	1	0	1	2	3	2	1	2	4	3	4	5	6	7	8	8	9	9	86
V_7	3	2	3	1	2	1	0	1	2	3	2	3	5	4	5	6	7	8	9	9	10	10	96
V_8	4	3	4	2	3	2	1	0	1	2	3	4	6	5	6	7	8	9	10	10	11	11	112
V_9	5	4	5	3	4	3	2	1	0	1	2	3	5	4	5	6	7	8	9	9	10	10	106
V_{10}	6	5	4	4	3	2	3	3	1	0	1	2	4	3	4	5	6	7	8	8	9	9	96
V_{11}	5	4	3	3	2	1	2	3	2	1	0	1	3	2	3	4	5	6	7	7	8	8	80
V_{12}	6	5	4	4	3	2	3	4	3	2	1	0	2	1	2	3	4	5	6	6	7	7	80
V_{13}	8	7	6	6	5	4	5	6	5	4	3	2	0	1	2	3	4	5	6	6	7	7	102
V_{14}	7	6	5	5	4	3	4	5	4	3	2	1	1	0	1	2	3	4	5	5	6	6	82
V_{15}	8	7	6	6	5	4	5	6	5	4	3	2	2	1	0	1	2	3	4	4	5	5	88
V_{16}	9	8	7	7	6	5	6	7	6	5	4	3	3	2	1	0	1	2	3	3	4	4	96
V_{17}	10	9	8	8	7	6	7	8	7	6	5	4	4	3	2	1	0	1	2	2	3	3	106
V_{18}	11	10	9	9	8	7	8	9	8	7	6	5	5	4	3	2	1	0	1	1	2	2	118
V_{19}	12	11	10	10	9	8	9	10	9	8	7	6	6	5	4	3	2	1	0	2	3	1	136
V_{20}	12	11	10	10	9	8	9	10	9	8	7	6	6	5	4	3	2	1	2	0	1	3	136
V_{21}	13	12	11	11	10	9	10	11	10	9	8	7	7	6	5	4	3	2	3	1	0	4	146
V_{22}	13	12	11	11	10	9	10	11	10	9	8	7	7	6	5	4	3	2	1	3	4	0	146

Table A.2: Vertex transmission of Figure 8.

V	V_1	V_2	V_3	V_4	V_5	V_6	V_7	V_8	V_9	V_{10}	V_{11}	V_{12}	V_{13}	V_{14}	V_{15}	V_{16}	V_{17}	V_{18}	V_{19}	V_{20}	V_{21}	V_{22}	V_{23}	$\sum$
V_1	0	1	2	2	3	4	3	4	5	6	5	6	8	7	8	9	10	11	12	13	14	12	13	158
V_2	1	0	1	1	2	3	2	3	4	5	4	5	7	6	7	8	9	10	11	12	13	11	12	137
V_3	2	1	0	2	3	2	1	2	3	4	3	4	6	5	6	7	8	9	10	11	12	10	11	122
V_4	2	1	2	0	1	2	3	4	5	4	3	4	6	5	6	7	8	9	10	11	12	10	11	126
V_5	3	2	3	1	0	1	2	3	4	3	2	3	5	4	5	6	7	8	9	10	11	9	10	93
V_6	4	3	2	2	1	0	1	2	3	2	1	2	4	3	4	5	6	7	8	9	10	8	9	96
V_7	3	2	1	3	2	1	0	1	2	3	2	3	5	4	5	6	7	8	9	10	11	9	10	107
V_8	4	3	2	4	3	2	1	0	1	2	3	4	6	5	6	7	8	9	10	11	12	10	11	124
V_9	5	4	3	5	4	3	2	1	0	1	2	3	5	4	5	6	7	8	9	10	11	9	10	108
V_{10}	6	5	4	6	3	2	3	2	1	0	1	2	4	3	4	5	6	7	8	9	10	8	9	108
V_{11}	5	4	3	3	2	1	2	3	2	1	0	1	3	2	3	4	5	6	7	8	9	7	8	89
V_{12}	6	5	4	4	3	2	3	4	3	2	1	0	2	1	2	3	4	5	6	7	8	6	7	85
V_{13}	8	7	6	6	5	4	5	6	5	4	3	2	0	1	2	3	4	5	6	7	8	6	7	110
V_{14}	7	6	5	5	4	3	4	5	4	3	2	1	1	0	1	2	3	4	5	6	7	5	6	89
V_{15}	8	7	6	6	5	4	5	6	5	4	3	2	2	1	0	1	2	3	4	5	6	4	5	94
V_{16}	9	8	7	7	6	5	6	7	6	5	4	3	3	2	1	0	1	2	3	4	5	3	4	101
V_{17}	10	9	8	8	7	6	7	8	7	6	5	4	4	3	2	1	0	1	2	3	4	3	2	110
V_{18}	11	10	9	9	8	7	8	9	8	7	6	5	5	4	3	2	1	0	1	2	3	1	2	121
V_{19}	10	11	10	10	9	8	9	10	9	8	7	6	6	5	4	3	2	1	0	1	2	2	3	129
V_{20}	13	12	11	11	10	9	10	11	10	9	8	7	7	6	5	4	3	2	1	0	1	3	4	157
V_{21}	14	13	12	12	11	10	11	12	11	10	9	8	8	7	6	5	4	3	2	1	0	4	5	178
V_{22}	12	11	10	10	9	8	9	10	9	8	7	6	6	5	4	3	2	1	2	3	4	0	1	178
V_{23}	13	12	11	10	9	10	11	10	9	8	7	7	6	5	4	3	2	1	3	2	4	5	0	152

Table A.3: Vertex transmission of Figure 9.

V_1	V_2	V_3	V_4	V_5	V_6	V_7	V_8	V_9	V_{10}	V_{11}	V_{12}	V_{13}	V_{14}	V_{15}	V_{16}	V_{17}	V_{18}	V_{19}	V_{20}	V_{21}	V_{22}	V_{23}	V_{24}	V_{25}	V_{26}	V_{27}	V_{28}	V_{29}	$\sum$
0	1	2	2	3	4	4	5	5	6	6	7	7	8	9	9	10	10	11	12	13	14	14	15	16	17	17	18	18	269
1	0	2	2	3	4	4	5	5	6	6	7	7	8	9	9	10	10	11	12	13	14	14	15	16	17	17	18	18	263
1	1	0	1	2	3	3	4	4	5	5	6	6	7	8	8	9	9	10	11	12	13	13	14	15	16	17	17	18	256
1	1	2	0	2	2	2	3	3	4	4	5	5	6	7	7	8	8	9	10	11	12	12	13	14	15	15	16	16	213
1	1	2	2	0	2	3	3	4	4	4	5	5	6	6	7	8	8	9	9	10	11	12	13	13	14	15	16	16	243
1	1	1	2	2	0	2	3	3	3	3	4	4	5	6	6	7	7	8	9	10	11	11	12	13	14	14	15	15	192
1	1	2	2	2	2	0	3	3	3	3	4	4	4	5	5	6	6	7	8	9	10	10	11	12	13	13	14	14	177
1	1	2	2	3	3	3	0	4	4	4	5	5	5	6	6	7	7	8	9	10	11	11	12	13	14	14	15	15	200
1	1	2	2	2	3	3	3	0	4	4	5	5	5	6	6	6	6	7	8	9	10	10	11	12	13	13	14	14	185
1	1	1	2	2	2	2	3	3	0	3	4	4	4	5	5	5	6	7	8	9	9	10	11	12	12	13	13	13	162
1	1	1	2	2	2	3	3	3	3	0	4	4	4	4	5	5	6	6	6	7	8	8	9	10	11	11	12	12	153
1	2	2	3	3	3	4	4	4	4	5	0	5	5	5	6	6	7	7	8	8	8	9	9	10	11	12	12	13	189
1	1	2	2	2	2	3	3	3	3	4	4	0	4	5	5	5	6	6	7	7	7	7	8	9	10	10	11	11	148
1	1	2	2	2	3	3	3	4	4	4	5	5	0	5	5	6	6	6	7	7	7	8	8	8	9	9	9	9	148
1	1	1	2	2	2	3	3	3	4	4	4	5	5	0	5	6	6	6	6	7	7	8	8	9	9	9	10	10	155
1	1	2	2	2	3	3	3	4	4	4	5	5	5	0	6	6	6	7	7	7	8	8	8	9	9	9	9	9	148
1	1	2	2	2	3	3	3	3	4	4	4	5	5	5	6	0	6	7	7	7	7	8	8	8	8	9	10	10	145
1	1	2	2	2	3	3	3	4	4	4	5	5	5	6	6	6	0	7	7	7	7	8	8	9	9	10	11	11	142
1	1	2	2	2	3	3	3	4	4	4	5	5	5	6	6	6	7	0	7	7	8	8	8	8	9	10	10	11	144
1	1	2	2	2	2	3	3	3	4	4	5	5	5	6	6	6	7	7	0	8	8	8	8	9	9	10	11	11	152
1	1	1	2	2	3	3	3	4	4	4	5	5	5	6	7	8	8	9	0	9	10	10	11	11	12	13	13	13	174
1	2	2	3	3	4	4	4	5	5	5	5	6	6	6	7	8	9	9	10	10	0	11	11	12	13	14	15	15	205
1	1	2	2	2	3	3	3	4	4	4	4	5	5	6	7	8	9	9	10	10	11	0	11	12	12	13	14	14	189
1	1	2	2	2	3	3	3	3	4	5	5	6	6	7	8	9	10	10	11	11	12	12	0	13	13	14	15	15	206
1	2	2	3	3	3	4	5	5	6	7	7	8	8	9	10	11	12	12	13	13	14	14	15	0	15	16	17	17	252
1	1	1	2	2	2	3	4	4	5	6	6	7	7	8	9	10	11	11	12	12	13	13	14	14	0	15	16	16	214
1	2	2	3	3	4	5	6	6	7	8	8	9	9	10	11	12	13	13	14	14	15	15	16	16	17	0	18	18	275
1	1	1	2	2	3	4	5	5	6	7	7	8	8	9	10	11	12	12	13	13	14	14	15	15	17	18	0	17	248
1	2	2	3	3	4	5	6	6	7	8	8	9	9	10	11	12	13	13	14	14	15	15	16	16	17	18	18	0	275

Table A.4: Vertex transmission of Figure 10.

V_1	V_2	V_3	V_4	V_5	V_6	V_7	V_8	V_9	V_{10}	V_{11}	V_{12}	V_{13}	V_{14}	V_{15}	V_{16}	V_{17}	V_{18}	V_{19}	V_{20}	V_{21}	V_{22}	V_{23}	V_{24}	V_{25}	V_{26}	$\sum$
0	1	2	2	3	3	4	4	5	5	6	6	7	8	9	10	10	11	11	12	12	13	14	15	16	16	198
1	0	1	1	2	2	3	3	4	4	5	5	6	7	8	9	9	10	10	11	11	12	13	14	15	15	181
1	2	0	2	3	3	4	4	5	5	6	6	7	8	9	10	10	11	11	12	12	13	14	15	16	16	205
1	1	1	0	2	2	2	2	3	3	4	4	5	6	7	8	8	9	9	10	10	11	12	13	14	14	151
1	1	2	2	0	2	2	3	3	3	3	3	4	5	6	7	7	8	8	9	9	10	11	12	13	13	151
1	1	2	2	2	3	0	3	3	3	4	4	4	4	5	6	6	7	7	8	8	9	10	11	12	12	142
1	1	1	2	2	2	2	0	3	3	3	4	4	4	5	6	6	7	7	8	8	9	10	11	12	12	140
1	1	1	2	2	2	2	3	0	3	3	4	4	5	5	5	5	6	6	7	7	8	9	10	11	11	123
1	1	2	2	2	2	3	3	3	0	3	4	4	4	5	5	5	6	6	6	6	7	8	9	10	10	117
1	1	2	2	2	3	3	3	3	4	0	4	4	5	5	5	5	6	6	7	7	8	9	10	11	11	127
1	1	2	2	2	3	3	3	4	4	4	0	4	5	5	5	5	6	6	6	6	7	8	9	10	10	121
1	1	1	2	2	2	3	3	3	3	4	4	0	4	4	5	5	5	6	6	7	7	7	8	9	9	111
1	1	2	2	2	2	3	3	3	3	4	4	4	0	4	5	5	5	6	6	7	7	8	8	8	8	111
1	2	2	3	3	3	4	4	4	4	5	5	5	6	0	6	6	7	7	7	8	8	8	9	10	10	137
1	1	1	2	2	2	3	3	3	3	4	4	4	5	5	0	5	6	6	6	7	7	7	8	9	9	113
1	1	1	2	2	2	2	3	3	4	4	4	5	5	5	6	0	6	6	6	7	7	8	9	10	10	119
1	1	2	2	2	3	3	3	3	4	4	5	5	5	5	6	6	0	7	7	8	8	9	10	11	11	131
1	1	2	2	2	3	3	3	4	4	4	4	5	6	6	7	7	8	0	8	9	9	10	11	12	12	140
1	1	2	2	2	3	3	3	3	4	4	5	5	5	5	6	6	7	7	0	8	8	9	10	11	11	131
1	1	2	2	2	3	3	3	4	4	4	4	5	6	6	7	7	8	8	9	0	9	10	11	12	12	132
1	1	1	2	2	2	3	3	3	4	5	5	6	7	7	8	8	9	9	10	10	0	11	12	13	13	155
1	1	2	2	2	2	3	3	4	5	6	6	7	8	8	9	9	10	10	11	11	12	0	13	14	14	173
1	2	2	3	4	4	5	5	6	7	8	8	9	10	10	11	11	12	12	13	13	14	15	0	16	16	226
1	1	1	2	3	3	4	4	5	6	7	7	8	9	9	10	10	11	11	12	12	13	14	15	0	15	193
1	2	2	3	4	4	5	5	6	7	8	8	9	10	10	11	11	12	12	13	13	14	15	16	16	0	217